

ARTICLES

Lateral and Vertical Quantification of Spin-Coated Polymer Films on Silicon by TOF-SIMS, XPS, and AFM

K. Norrman,^{*,†} K. B. Haugshøj,[‡] and N. B. Larsen[†]*The Danish Polymer Centre, Risø National Laboratory, DK-4000 Roskilde, Denmark, and Centre for Surface Analysis, Danish Technological Institute, DK-2630 Taastrup, Denmark**Received: January 11, 2002; In Final Form: July 22, 2002*

PMMA and PVC were spin coated on silicon wafers using a range of polymer concentrations. This resulted in a corresponding range of film thicknesses and, for ultrathin film layers, various degrees of surface coverage. The thickness was determined by AFM profilometry and was used to correlate the time scale of a dynamic TOF-SIMS depth profile analysis to a depth scale. The degree of surface coverage was determined from AFM imaging and was used to correlate polymer secondary-ion yields of a static TOF-SIMS analysis to the degree of surface coverage. TOF-SIMS imaging was found to be inferior to AFM imaging with regard to determining the degree of surface coverage of polymers on silicon surfaces. PVC and PMMA both form separated domains on silicon when using spin-coating solutions with a polymer concentration below a material-dependent threshold. In the intermediate concentration range between domain formation and complete surface coverage, networks form. At low concentrations, the deposited polymer material was heterogeneously distributed in the plane of the film as well as vertically to the substrate, resulting in relatively thick hillocks distributed over a limited surface area. At higher concentrations, where network formation is observed, the polymer is heterogeneously distributed in the plane of the film with a large degree of surface coverage, and the average small thickness of the polymer network is fairly constant. A linear correlation was observed between the secondary-ion yield and the degree of surface coverage for both PVC and PMMA, which constitutes the calibration curves for the lateral quantification.

1. Introduction

TOF-SIMS (time of flight-secondary ion mass spectrometry) is a powerful tool for obtaining chemical information about surfaces.^{1,2} Static TOF-SIMS (hereafter termed TOF-SIMS) produces a mass spectrum of species found in the outer few monolayers of the surface. A lot of valuable information can be extracted from a surface mass spectrum (e.g. molecular and structural information). If a sputter gun is used in combination with the TOF-SIMS analysis, a depth profile can be obtained for any species detected by the mass spectrometer. This is known as dynamic TOF-SIMS.

TOF-SIMS is a technique based on mass spectrometry and is therefore said not to be a quantitative technique, whereas XPS (X-ray photoelectron spectroscopy) has proven to be quantitative. XPS measures the surface element composition and is often used as an alternative or complementary technique when quantification is needed.² However, XPS probes deeper into the surface (5–10 nm) than TOF-SIMS (~1 nm), which makes it difficult, but not impossible, to correlate XPS data with TOF-SIMS data. This discrepancy in the probing depth is often reduced by performing the XPS analysis at a grazing angle.

The fundamental reason for mass spectrometry not being directly quantitative is that a given species may have varying response factors (i.e. produce different signal intensities per unit of matter). For surface mass spectrometry, it makes more sense to use the related property termed the secondary-ion yield, which is the number of secondary ions detected relative to the number of impinging primary ions. Basically, the secondary-ion yield must be the product of the desorption probability and the ionization probability, which both depend on various factors (e.g., the identity of the elements, and in case of molecules, the chemical structure the elements form, the surface topography, and to complicate things even more, the matrix could influence the response factors. Matrix effects may affect the signal intensities from the same compound on different substrates profoundly, which is one of the major problems when trying to use TOF-SIMS quantitatively).

Despite TOF-SIMS not being a quantitative technique, extensive efforts have been spent on finding ways to use TOF-SIMS quantitatively.¹ They all employ calibration curves to make TOF-SIMS quantitative. If the calibration curve is found to be linear, it usually suggests that there are no matrix effects involved. However, a nonlinear calibration curve is equally good regardless of the shape of the curve and is therefore applicable. One could argue that a quantification based on a calibration curve should be termed semiquantitative. However, as this

* Corresponding author. E-mail: kion.norrman@risoe.dk. Fax: (+45)-46-77-47-91.

[†] Risø National Laboratory.

[‡] Danish Technological Institute.

distinction is irrelevant to the applications, we will consistently use the term quantitative in the rest of this paper.

Galuska^{3–5} has, in a series of articles, described work regarding the quantification of copolymers and blends mainly by the use of TOF-SIMS. As part of this work, he studied the surface morphology of copolymers of ethylene and vinyl acetate³ and copolymers of ethylene and methyl acrylate.⁴ He also managed to quantify the proportion of ethylene and propylene in copolymers of these molecules,⁵ which is noteworthy since this copolymer is entirely hydrogen- and carbon-based and structurally and chemically very similar.

Li et al.⁶ studied the time-dependent morphology change of a spin-coated condensation polymer of bisphenol A and 1,8-dibromooctane. The morphology was monitored by AFM imaging. TOF-SIMS imaging revealed the bromine end-groups initially to be distributed homogeneously at the surface of the amorphous film. During crystallization, the end groups preferentially accumulate at the edges and boundaries of the spherulites.

Jackson and Short⁷ used TOF-SIMS to study the morphology of PVC/PMMA blends cast from tetrahydrofuran (THF). They found the bulk and surface morphology to be the same. Briggs et al.^{8–10} studied equivalent blends and found from XPS imaging and TOF-SIMS imaging that the bulk morphology extends almost to the surface, with the outer ~1-nm layer consisting of homogeneously distributed PMMA.

Leeson et al.¹¹ studied PMMA that was spin and solution coated on aluminum substrates. They used PMMA standards with various molecular weights and studied the effects of molecular weight and film thickness on SIMS spectra. They found that the total negative-ion count decreases and that some intensity ratios changed for higher molecular weights and for larger film thicknesses, which was attributed to (i) the original surface end-group concentration that decreases for increasing molecular weight and (ii) the original surface end-group concentration that increases for smaller film thicknesses.

Muddiman et al.¹² studied polystyrene on etched silver. They correlated secondary-ion yields with ISS (ion scattering spectroscopy) data and XPS data. ISS has an inherent extremely high surface sensitivity (one atomic layer) that allows for the measurement of the submonolayer surface coverage of a polymer on a substrate. XPS analysis may be used to estimate the mean thickness of the polymer layer (if it is less than ~10 nm). These authors found that the TOF-SIMS secondary-ion yield increases with surface coverage up to ca. 50% and then drastically decreases for coverages greater than 55%. XPS analysis showed that polystyrene forms a multilayer structure that is at least five layers thick for the concentration range between 1 $\mu\text{g/mL}$ and 50 mg/mL (solution adsorption).

Our current work is similar to work by Muddiman et al.¹² However, we target a more detailed analysis of the correlation between the spatially averaged measurable quantities (secondary-ion yield and elemental composition for TOF-SIMS and XPS, respectively) and the in-plane as well as out-of-plane distribution of deposited material. We have chosen thin films of PMMA and PVC on silicon as our model polymers because of their surface-relevant difference in hydrophilicity and the presence of different heteroatoms that are useful for both SIMS and XPS analysis. PMMA and PVC are spin coated on silicon wafers using a range of polymer concentrations, resulting in a corresponding range of film thicknesses. Low polymer concentrations produce submonolayers with a range of surface coverage. The layer thickness is determined from AFM (atomic force microscopy) profilometry, which is then used to correlate the time

scale of a dynamic TOF-SIMS depth-profile analysis to a depth scale. The degree of surface coverage is determined from AFM imaging, which is then used to correlate the polymer secondary-ion yields from a static TOF-SIMS analysis to a degree of surface coverage.

2. Experimental Section

2.1. Sample Preparation. PMMA ($M_w = 70 \text{ kg/mol}$, $M_w/M_n = 2.09$) was dissolved in chloroform, and PVC ($M_w = 80 \text{ kg/mol}$, $M_w/M_n = 1.7$), in a mixture of cyclohexanone and THF (3:2 v/v). Solutions were prepared in the concentration range of 1–10 000 $\mu\text{g/mL}$ by serial dilution. All of the chemicals that were used were products of Fluka (Buchs, Switzerland) and Aldrich (Milwaukee, WI) and were used without further purification.

We used silicon wafers (100, single side polished) purchased from Topsisil (Frederiksund, Denmark). Ultrapure water was supplied by a Milli-Q system from Millipore (Boston, MA). The wafers were cut into suitable sizes ($\sim 1 \times 1 \text{ cm}^2$) and cleaned by sonication in ethanol/water (1:1 v/v) for 15 min. The substrate was oxidized in a mixture of hydrogen peroxide (30% w/v) and sulfuric acid (96% w/v, 20:80 v/v) for 10 min at 120 °C. *Caution: this mixture should be used with extreme care because of its oxidizing power and risk of detonation.*¹³ The wafers were washed with copious amounts of water, blow dried with dry carbon dioxide, and immediately spin coated with the various polymer solutions. The silicon wafers cannot be stored but must be spin coated within a few hours after the cleaning procedure. The result of the spin-coating process is very dependent on the cleanliness of the silicon wafers. The silicon wafers were spin coated at 4000 rpm for 60 s. It was necessary to spin coat the silicon wafers in a clean room (class 100) because deposited impurities from the atmosphere are detrimental to the spin-coating process.

2.2. AFM. The spin-coated silicon wafers were analyzed with a Dimension 3000 AFM from Digital Instruments (Santa Barbara, CA) operating in tapping mode using Ultra-Sharp (NT-MDT, Moscow, Russia) or Super-Sharp silicon (NanoSensor, Wetzlar-Blankenfeld, Germany) tips. The degree of surface coverage was calculated on the basis of imaged surface areas between $5 \times 5 \mu\text{m}^2$ and $50 \times 50 \mu\text{m}^2$ depending on what was most representative in terms of resolution and statistical accuracy (512×512 pixels, 0.2-Hz scan frequency). The AFM images were processed by a threshold function to disregard intermediate height levels. Because of very consistent trends in the AFM imaging results, only one measurement was acquired for each sample.

The thicknesses of the spin-coated polymer layers were measured under the same imaging conditions ($50 \times 20 \mu\text{m}^2$ area) by AFM profilometry across a scratch made in the polymer layer by a brass pin. These measurements were repeated three times at different locations, and the average value was used.

2.3. XPS. The XPS analyses were performed using a Sage 100 (SPECS, Berlin, Germany) operated at a pressure of 10^{-7} Torr. The analysis was performed at a take-off angle of 90° from the surface plane upon emission by an Al X-ray source operated at 300 W. Polymers are known to be degraded to some extent by X-ray irradiation.² Since the analysis area covers most of the sample, the samples were not used for further analysis after XPS. For these reasons, the XPS measurements were performed last. Because of the destructive nature of the XPS analysis combined with the fact that very consistent trends were obtained, only one measurement was acquired for each sample.

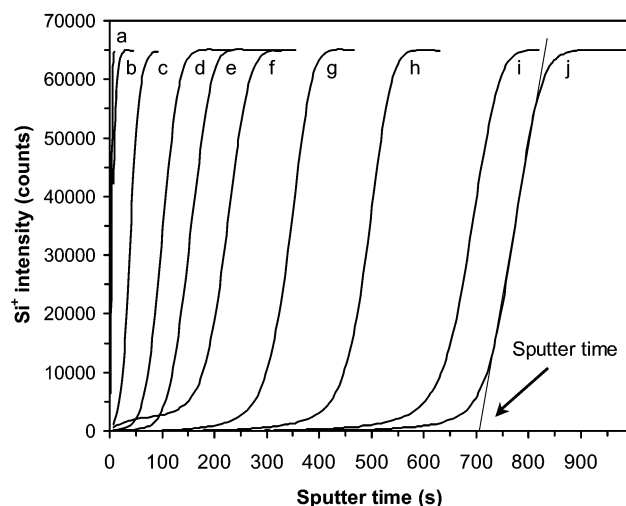


Figure 1. Sputter profiles for spin-coated PVC on silicon using Si^+ as a marker for the substrate. The curves correspond to polymer concentrations of (a) 1000, (b) 2000, (c) 3000, (d) 4000, (e) 5000, (f) 6000, (g) 7000, (h) 8000, (i) 9000, and (j) 10 000 $\mu\text{g/mL}$. Each sample was analyzed three times at different locations, and the average value was used.

2.4. TOF-SIMS. The TOF-SIMS analyses were performed using a TOF-SIMS IV (Ion-ToF GmbH, Münster, Germany) operated at a pressure of 2×10^{-8} Torr (with sample). Fifteen-nanosecond pulses of 15-keV Ga^+ (primary ions) were bunched to form ion packets with a nominal temporal extent of <0.9 ns at a repetition rate of 10 kHz, thus yielding a target current of 1 pA. These primary ion conditions were used to scan a $100 \times 100 \mu\text{m}^2$ area of the sample for 30 s, which corresponds to an ion dose 1.9×10^{12} ions/ cm^2 (below the static limit). A flood gun was used to minimize built-up charge at the surface. Desorbed secondary ions were accelerated to 2 keV, mass analyzed in the flight tube, and postaccelerated to 10 keV before detection. Each sample was analyzed five times at different locations, and the average value was used.

The same analytical conditions for the gallium gun were used in the depth-profiling process. SF_5^+ (1 keV) was used for the sputtering at a target current of 0.5 nA, which is sufficient to sputter off part of the polymer layer. A $300 \times 300 \mu\text{m}^2$ area of the sample was sputtered, and the central $100 \times 100 \mu\text{m}^2$ area was analyzed. Each sample was analyzed three times at different locations, and the average value was used.

3. Results and Discussion

The silicon wafers were spin coated using polymer solutions in the concentration range between 1 and 10 000 $\mu\text{g/mL}$. The higher the polymer concentration used, the thicker the layer. It is difficult to define a polymer monolayer, as polymer molecules tend to entangle and fold up in coiled conformations, thus producing a lower thickness limit for a stable continuous polymer film of a substantial number of polymer chain diameters. However, it was almost impossible to measure the layer thickness of the 1000 $\mu\text{g/mL}$ samples with AFM or TOF-SIMS, thus the 1–2000 $\mu\text{g/mL}$ samples were used for lateral quantification and the 1000–10 000 $\mu\text{g/mL}$ samples were used for vertical quantification.

3.1. Vertical Quantification. Depth profiles for the spin-coated silicon wafers are shown in Figures 1 and 2. Even though charge compensation was employed during the analyses, the built-up charge caused the polymer signals to decay within seconds. The substrate signal, Si^+ , was used instead to monitor when the entire polymer had been eroded.

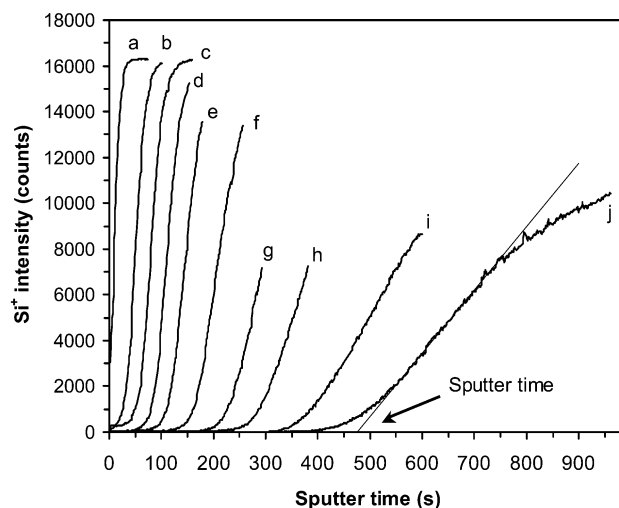


Figure 2. Sputter profiles for spin-coated PMMA on silicon using Si^+ as a marker for the substrate. The curves correspond to polymer concentrations of (a) 1000, (b) 2000, (c) 3000, (d) 4000, (e) 5000, (f) 6000, (g) 7000, (h) 8000, (i) 9000, and (j) 10 000 $\mu\text{g/mL}$. Each sample was analyzed three times at different locations, and the average value was used.

We have to select a workable definition of the sputter time required to erode all of the polymer. The choice of definition is not critical as long as it is being applied consistently because the time scale needs to be converted via a calibration to a depth scale anyway. We have chosen to extrapolate the tangent at the inflection point of the Si^+ intensity curve to the time axis and to use this value as our sputter time (see Figures 1 and 2).

When the profiles for PVC and PMMA are compared, several differences are evident. Even though the samples were analyzed under the same conditions, the maximum silicon signal intensities for the two polymers differ by a factor of 4. This could be due to interlayer mixing. There will always be some material implanted into deeper layers because of the sputter/analysis process; this material will eventually end up in the substrate, in this case, the silicon. When the substrate is reached, it will be contaminated by low levels of other species, which could result in a matrix effect. This is supported by the mass spectra of the regions with maximum silicon intensity, which in all cases contain a large variety of peaks originating from organic species (presumably degraded polymer), inorganic and organic sulfur, and fluorine species (SF_5^+ reacting with the polymer and substrate). The distribution of the peaks originating from the contamination in question is different when PVC and PMMA are compared, which suggests that the matrix effect could be different for the two systems. The profile shapes for the two polymers also differ, especially at high sputter times. The PVC profiles are all more or less similar in shape, whereas the PMMA profiles change shape across the sputter-time axis (i.e. they become less steep at longer sputter times).

Ideally, the silicon signal should appear at one particular sputter time and go to maximum intensity instantly, but the larger escape depth of silicon atoms or ions (it is not well-known where the ionization takes place) is likely to cause detection of silicon before all of the polymer has been eroded. The smaller the species, (e.g., small atoms), the greater the likelihood is for desorbing/escaping from subsurface layers.¹⁴ Poor sputter-depth resolution could in principle also be a contributing factor. However, we have tested the depth resolution on a gold/chromium multilayer sample with known layer thicknesses and have found a depth resolution of ~ 1 nm when using SF_5^+ at 1 keV as the sputter ion. Since this test was performed on a metal

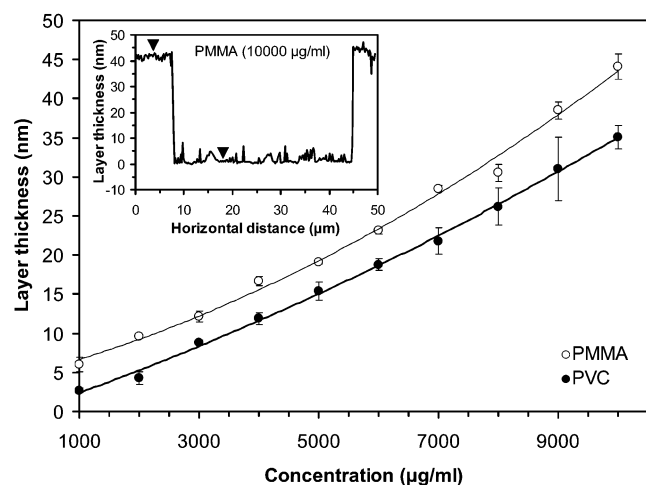


Figure 3. Layer thickness (measured by AFM) vs concentration. Each point is an average of three measurements with a corresponding standard deviation. The AFM profile shown is that of an applied scratch in a PMMA film on silicon produced from a 10 000 $\mu\text{g/mL}$ spin-coating solution. The thickness is determined from the vertical distance between the two marked locations.

sample, we can of course not expect to obtain the same depth resolution for a polymer. It will most likely be worse, but probably not to the extent that it could explain the very early appearance of the silicon signal. One could argue that silicone oil contamination on the surface could be contributing to this phenomenon. Silicone oil is easily recognized from its “fingerprint” TOF-SIMS mass spectrum, and since the levels present are negligible, this is most likely not an important factor.

In Figure 3, the layer thickness (measured by AFM) is plotted against the concentration of the polymer solutions. As expected, the layer thickness increases for higher concentrations. The uncertainty in the layer thickness is larger for higher concentrations, which is probably one explanation for the larger uncertainty in the sputter time at higher concentrations. An AFM profile of an applied scratch is shown as part of Figure 3 for PMMA at 10 000 $\mu\text{g/mL}$. Measurement of the height difference between the polymer surface and the silicon surface can be done very accurately (uncertainty less than 5%), so the uncertainties in the layer thicknesses are caused only by thickness variations across the polymer surface.

Plotting the layer thickness against the sputter time (Figure 4) produces the desired calibration curves for the vertical quantification. From the nonlinearity, we can conclude that the sputter rate (Figure 5) varies with the integrated ion fluence, possibly because of a combination of insufficient charge compensation and chemical modification of the polymer induced by the sputter process (e.g. cross linking and/or bond cleavage) or because of interlayer mixing. Both of these phenomena could result in a matrix effect influencing the ion yield. The sputter rates decrease for thicker layers and seem to level out toward a constant rate of ~ 0.05 nm/s for PVC and ~ 0.09 nm/s for PMMA. It should be noted that the absolute rate values are affected by the choice of definition for the sputter time but that the qualitative trend should be unaffected by this. It is not clear whether the sputter rate on the polymers changes because of induced chemical modification within the polymer or because of interlayer mixing. It could be argued that to clarify this the experiment should be performed in reverse order (i.e., sputtering for a time less than what it takes to detect silicon and then measuring the depth of the crater by AFM profilometry). However, a direct measurement of the depth of a sputter crater is extremely difficult for the conditions in question (large sputter

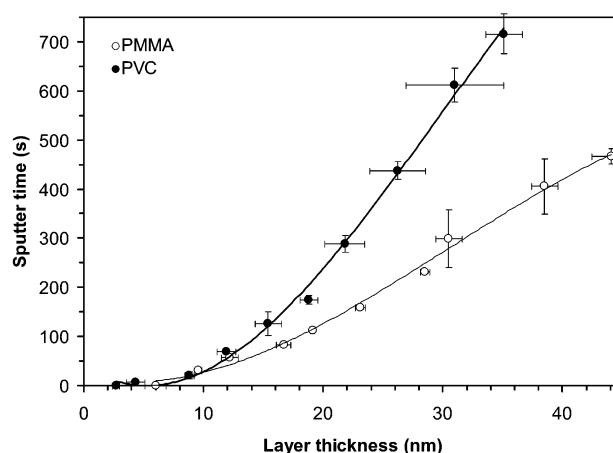


Figure 4. TOF-SIMS sputter time vs layer thickness (measured by AFM). Each point is an average of three measurements with a corresponding standard deviation. This is the calibration curve for the lateral quantification.

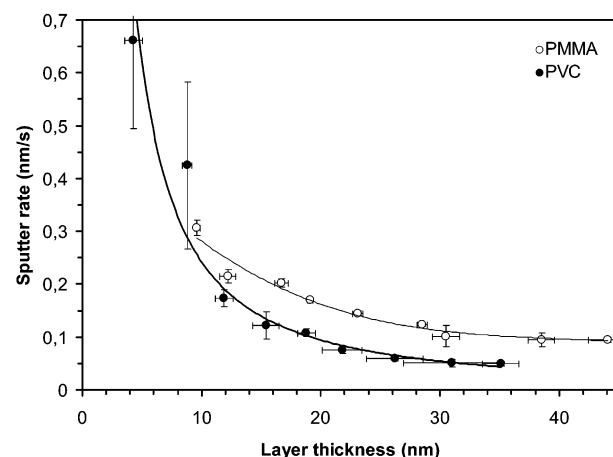


Figure 5. TOF-SIMS sputter rate vs layer thickness (measured by AFM). Each point is an average of three measurements with a corresponding standard deviation.

area, $300 \times 300 \mu\text{m}^2$, and small depth, $\sim 1\text{--}10$ nm), so instead we chose to measure the sputter time accurately to obtain reproducible polymer film thicknesses. It is not important for the sputter rates to be accurate when using this methodology for actual thickness measurements since the quantification is based on a calibration.

3.2. Lateral Quantification. PMMA and PVC have different surface energies, PMMA being more hydrophilic and PVC being more hydrophobic. Partly because of this difference, the two polymers are expected to interact differently with the hydrophilic silicon oxide surface, which in turn will affect the polymer distribution in the lateral plane.

In the lower concentration range, PVC and PMMA form domains, whereas both form continuous layers of increasing thickness at higher concentrations. TOF-SIMS imaging (200-nm beam diameter) and AFM imaging were performed on the same PVC sample (100 $\mu\text{g/mL}$) and across the same area size ($50 \times 50 \mu\text{m}^2$) but on different locations on the surface. The resulting images are compared in Figure 6. The AFM image was transformed into a binary image (via a threshold function to disregard intermediate height levels) where black represents the polymer and white, the substrate. The TOF-SIMS image (based on chemical information) is a gray-scale image where black represents a high polymer intensity (Cl^- in this case), gray represents less intensity, and white represents zero intensity. As is evident, the image is blurred and has weak contrast

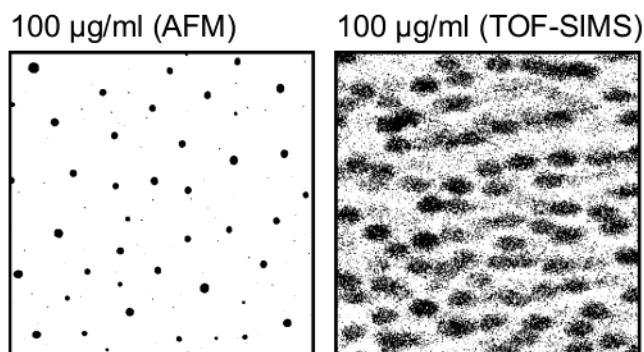


Figure 6. TOF-SIMS and AFM images of spin-coated PVC (100 $\mu\text{g/mL}$) on silicon. In each case, an area of $50 \times 50 \mu\text{m}^2$ was analyzed. Black represents PVC, and white represents the substrate. The AFM image has been processed by a threshold function to disregard intermediate height levels. The TOF-SIMS imaging was performed using 25-keV Ga^+ (200-nm beam diameter) in burst alignment mode, producing a target current of 0.7 pA.

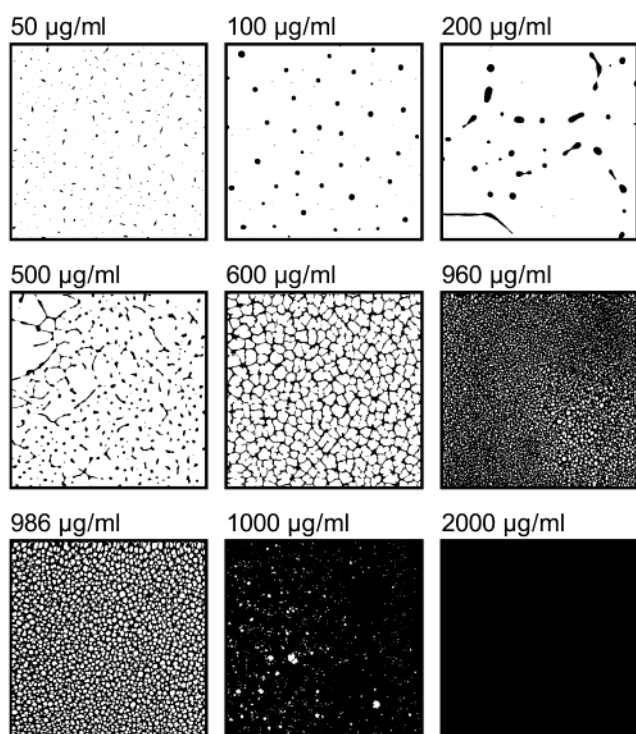


Figure 7. AFM images of spin-coated PVC on silicon using a range of PVC concentrations. In each case, an area of $50 \times 50 \mu\text{m}^2$ was analyzed. The images have been processed by a threshold function to show PVC in black and the substrate in white.

between polymer and substrate. TOF-SIMS is a very sensitive technique, especially with respect to the chloride ion, which is the ion used as a marker for PVC. Chlorine-containing surface contamination and residual PVC combined with possible matrix effects are probably the reason for the lack of contrast and the blurriness in the TOF-SIMS image. It cannot be transformed into a binary image because of difficulties in defining a threshold between polymer and substrate. TOF-SIMS imaging is clearly inferior to AFM imaging with regard to determining the lateral distribution of polymers on silicon surfaces.

Binary AFM images are shown in Figure 7 for selected PVC samples. The domains are very distinct at low concentrations. At approximately 500 $\mu\text{g/mL}$, a change in material distribution takes place, resulting in network formation instead of isolated domains. For higher concentrations, the network gradually increases in density so that a polymer layer with holes is formed.

Somewhere between 1000 and 2000 $\mu\text{g/mL}$ a 100% degree of surface coverage is obtained.

The same qualitative behavior is observed for PMMA on the silicon surfaces. However, because of the difference in physical properties, the previously discussed concentration windows are not expected to be the same as for PVC. The PMMA domains are smaller relative to the PVC domains, and the PMMA network is finer structured compared to the PVC network. Consequently, TOF-SIMS imaging (having the inferior lateral resolution) on submonolayers of PMMA is even more difficult compared to PVC. Because of the very small PMMA domains, it was not possible to obtain reliable AFM results for concentrations lower than 10 $\mu\text{g/mL}$.

The accuracy of an analysis of the surface coverage by AFM is inherently limited by the finite size of the AFM tip that will cause a broadening of surface features. This effect will be more pronounced the longer the contour line and the steeper the sidewalls of the surface features. It will obviously also depend on the geometry of the AFM tip used. The hillocks and networks observed in our studies are found to have very gentle sidewall slopes. Furthermore, the use of ultrasharpened tips (Super-Sharp silicon, nominal radius less than 2 nm) on selected critical samples did not cause substantial variations in the measured surface coverage compared to normal AFM tips (nominal radius less than 10 nm). Consequently, the effect of AFM tip broadening is considered to be of minor importance in this work.

The PVC and PMMA samples were prepared over a very broad concentration range (1–10 000 $\mu\text{g/mL}$) to ensure that the concentration windows for which the network formation takes place were reached. Additional samples were prepared for PVC in the concentration range corresponding to network formation (500–1000 $\mu\text{g/mL}$). Unfortunately, it was not possible to reproduce the correlation between the concentration and the degree of surface coverage accurately. We suggest that the spin-coating process is very sensitive toward very small differences in either the polymer concentration or the solvent composition for the ultrathin polymer films used in this work. In the following discussion, all correlations to the concentration are therefore made entirely with samples from the same spin-coating batch. This also explains the discrepancy between the 960 and 986 $\mu\text{g/mL}$ samples in Figure 7.

There is no obvious TOF-SIMS marker for PMMA, so three potentially useful markers were chosen: (i) the ion with an element composition of $\text{C}_{10}\text{H}_{16}\text{O}_4^+$, which is equivalent to the PMMA dimer, (ii) $\text{C}_5\text{H}_9\text{O}_2^+$, which is equivalent to the protonated monomer, and (iii) $\text{C}_4\text{H}_5\text{O}^+$, which is equivalent to a monomer that has lost a methoxy group. The smaller the ions, the less specificity that can be expected (i.e., they can be formed via various reaction paths and originate from different parts of the polymer structure). One would therefore expect the high-mass ions to be a better marker for the polymer, especially when looking for potential structural changes. The secondary-ion yields for these three PMMA markers are plotted against the concentration in Figure 8. As is evident, the secondary-ion yield for the largest ion, $\text{C}_{10}\text{H}_{16}\text{O}_4^+$, increases slowly until $\sim 90 \mu\text{g/mL}$, after which it starts to increase drastically until $\sim 1500 \mu\text{g/mL}$ and then finally decreases. This suggests that a structural change is taking place for PMMA between ~ 90 and $\sim 1500 \mu\text{g/mL}$, which is in good agreement with the aforementioned concentration window, where network formation takes place. The curve break is less pronounced when monitoring the smaller ion, $\text{C}_5\text{H}_9\text{O}_2^+$, and not observable at all when the smallest of the three markers, $\text{C}_4\text{H}_5\text{O}^+$, is monitored, in good agreement with the expectations presented above. The maximum second-

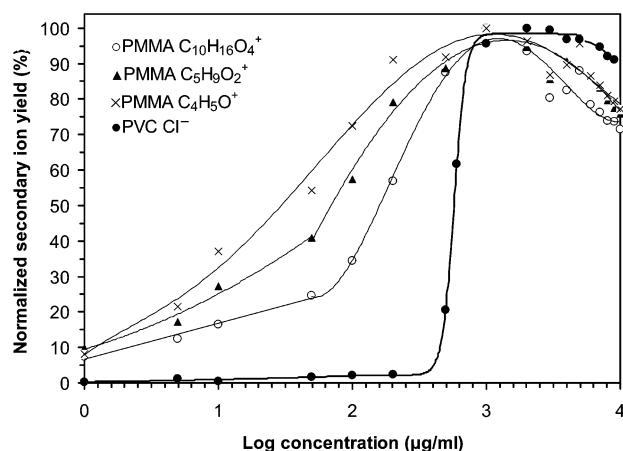


Figure 8. TOF-SIMS secondary-ion yield vs concentration. Each point is an average of five measurements. The standard deviations were omitted for clarity.

ary-ion yield is observed at $\sim 1000 \mu\text{g/mL}$ for both polymers, suggesting similar concentrations for what corresponds to 100% surface coverage. This is supported by the similarity in the polymer thicknesses at $1000 \mu\text{g/mL}$ ($6.0 \pm 0.9 \text{ nm}$ for PMMA and $2.7 \pm 0.3 \text{ nm}$ for PVC, measured by AFM profilometry). Above $\sim 2000 \mu\text{g/mL}$, the secondary-ion yield decreases slightly for both polymers, as expected. Two (possibly competing) factors could explain this phenomenon: (i) When the polymer layer becomes thicker, its surface will become less conductive because of the increasing distance to the conducting substrate. Built-up charge due to incomplete charge compensation will then become more dominating, which in turn will decrease the secondary-ion yield. (ii) The sputter process will chemically modify the polymer (e.g., degradation (bond cleavage/cross-linking), introduction of gallium and SF_5^+ reaction products, and interlayer mixing). Such modifications could induce a matrix effect and thereby possibly affect the substrate signal intensity.

The chloride ion is an obvious choice as a marker for PVC. One could argue that the chloride ion, being an atomic species, will have a significantly different information depth¹⁴ compared to the selected large PMMA fragment ion $\text{C}_{10}\text{H}_{16}\text{O}_4^+$. However, since each data set was individually calibrated against AFM data, it is not important in this context where we aim at determining the surface coverage of a single polymer material. Consequently, the development of the secondary-ion yields with the coverage of different polymers should not be compared. The secondary-ion yield of the chloride ion is plotted against the concentration in Figure 8. From 1 to $\sim 400 \mu\text{g/mL}$, there is a subtle increase in the secondary-ion yield, and between ~ 400 and $\sim 2000 \mu\text{g/mL}$, there is a drastic increase that corresponds to the aforementioned concentration window, where network formation takes place.

XPS data was correlated to the concentration (Figure 9). As is evident, a break in each curve, which happens to correspond to the aforementioned concentration windows, where network formation takes place, is observed. We know from Figure 8 that the secondary-ion yield for the marker ions starts to increase drastically at this same concentration, so we can expect the degree of surface coverage to start increasing at the same concentrations. AFM analysis of the degree of coverage supports this hypothesis (see Figure 10).

Why does the degree of surface coverage increase drastically from the concentration that corresponds to incipient network formation? It is tempting to conclude that more material is being deposited from this point, but that is not the case. The

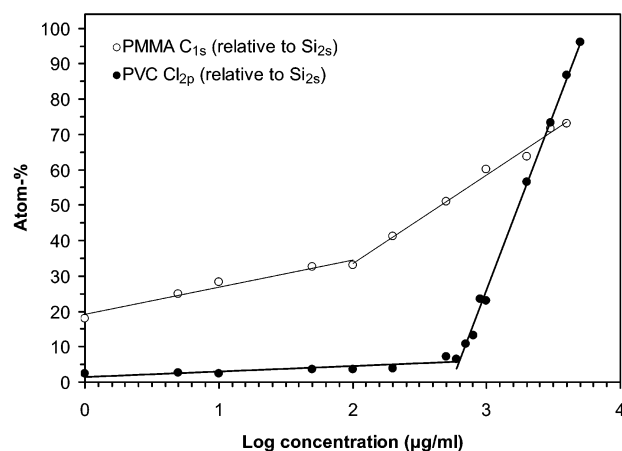


Figure 9. $\text{C}/(\text{C} + \text{Si})$ and $\text{Cl}/(\text{Cl} + \text{Si})$ compositions determined by XPS vs layer thicknesses measured by AFM. C_{1s} , Cl_{2p} , and Si_{2s} peaks were used for quantification. XPS results are based on single measurements.

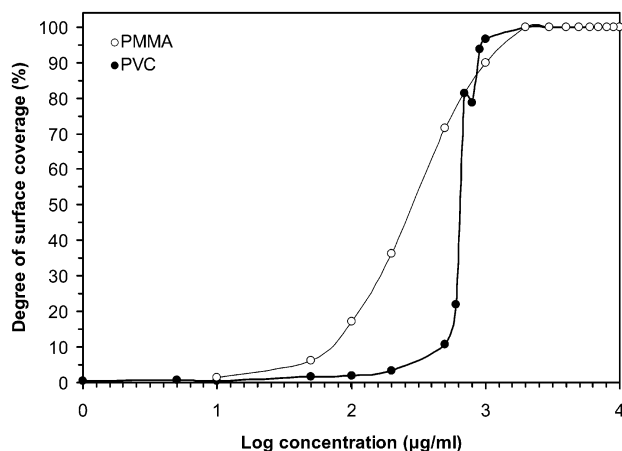


Figure 10. Degree of surface coverage (measured by AFM) vs concentration. AFM image results are based on single measurements. It was not possible to obtain reliable AFM image results for PMMA below $10 \mu\text{g/mL}$.

submonolayer domains and network have different heights depending on the concentration used. The maximum “layer” thickness (the “layer” being either the domains or network) is plotted against the concentration in Figure 11. As an example, the maximum thickness for PVC is seen to increase from a few nanometers to 20 nm in the concentration range between 1 and $200 \mu\text{g/mL}$ (the value for $500 \mu\text{g/mL}$ (40 nm) is regarded as an outlier point and was therefore excluded from the plot) and then decreases steeply to the few nanometers found throughout the polymer networks. This observation stresses that the degree of surface coverage is a poor measure of the amount of material deposited. On the basis of the original AFM images, we have calculated the amount of material per area by (i) volume integration of heights greater than 1 nm above the substrate level and (ii) adding the volume of the extruded area at 1 nm above the substrate to the substrate level. The calculated polymer volume was scaled by the size of the AFM image that was examined to yield an effective layer thickness (Figure 12). We find the expected power law dependence between the amount of polymer deposited and the concentration in the spin-coating solution. Neither polymer shows an increase in the amount deposited on the surface at the concentration that corresponds to incipient network formation. At low concentrations, the polymer is heterogeneously distributed in the lateral as well as the vertical direction, resulting in relatively thick domains

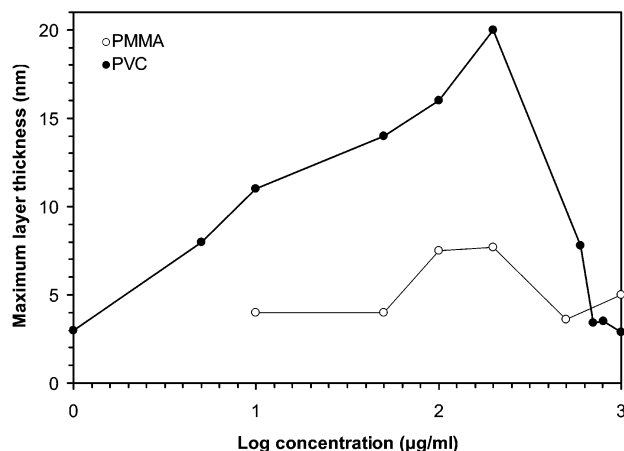


Figure 11. Maximum layer thickness (measured by AFM) vs concentration. Maximum layer thickness refers to the maximum thickness measured for any part of the network or for any single domain. The value for 500 $\mu\text{g/mL}$ (40 nm) is regarded as an outlier point and was therefore excluded from the plot.

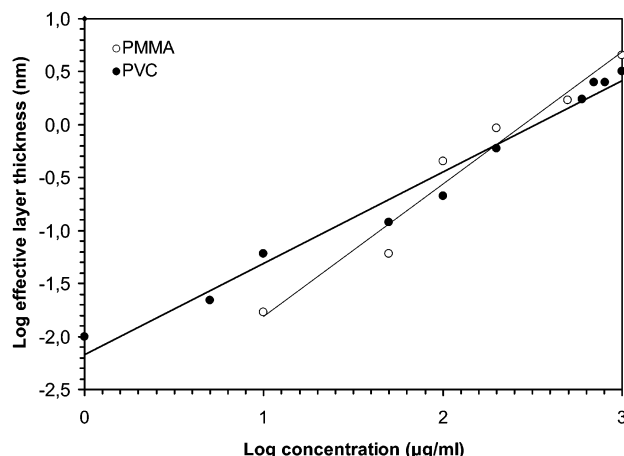


Figure 12. Effective layer thickness (measured by AFM) vs concentration. Effective layer thickness was calculated from the integrated volume of polymer. Effective layer thickness refers to the layer thickness that the material present on the surface would produce if it was homogeneously distributed. The fitted lines reflect a power law dependence of the amount of polymer on the concentration, as normally observed for spin coating. PVC: The slope is 0.9, and the correlation coefficient is 0.989. PMMA: The slope is 1.2, and the correlation coefficient is 0.981.

distributed over a limited surface area. At higher concentrations, when the network starts to form, it is more favorable to distribute the polymer in the lateral plane rather than normal to the surface plane, resulting in a relatively thin network with a large degree of surface coverage.

We can now explain the trends in the XPS and TOF-SIMS measurements on ultrathin films. If the TOF-SIMS results on PVC in Figure 8 and the AFM thickness measurements in Figure 10 are compared with respect to the submonolayer concentration ranges, it is evident that the plotted curves are (within the accuracy of the measurements) superimposable. Two conclusions can be made on the basis of this observation: (i) the probe depth is (not surprisingly) very small and (ii) there are no detectable (or significant) matrix effects. The secondary-ion yield for the marker ions appears to depend mainly or only on the degree of surface coverage. For PMMA, this is true only for the $\text{C}_{10}\text{H}_{16}\text{O}_4^+$ ion.

Whereas TOF-SIMS has a very small probe depth, XPS probes significantly deeper. However, the XPS probe depth is not linear; it decreases exponentially with depth. Approximately

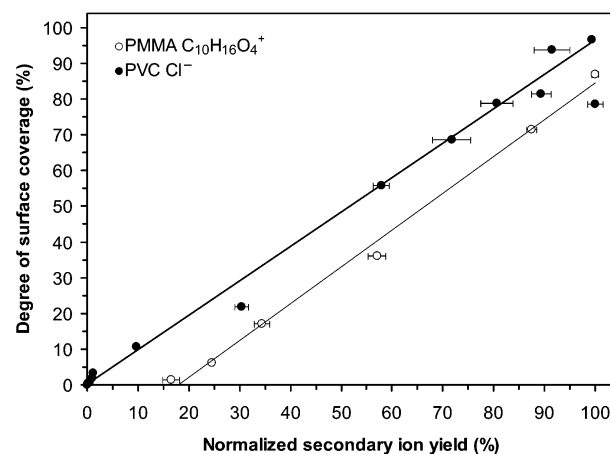


Figure 13. Degree of surface coverage (measured by AFM) vs TOF-SIMS secondary-ion yield. The secondary-ion yields are averages of five measurements with a corresponding standard deviation. AFM image results are based on single measurements. PVC: The slope is 0.96, the intercept is zero, and the correlation coefficient is 0.997. One outlier point at 100% normalized secondary-ion yield was excluded in the linear regression for PVC. PMMA: The slope is 1.03, the intercept is -18% , and the correlation coefficient is 0.998.

70% of the signal originates from the upper 2.5–3.0 nm of the surface. In the low-concentration regime, the increase in the polymer signal for higher concentrations is small because most of the extra polymer increases the height of the domains rather than the surface coverage. In other words, some of the polymer material is being discriminated in the XPS analysis. In the network concentration range, the degree of surface coverage is high, and the thickness is on the order where we can expect only minor discrimination, which results in a significant increase in the polymer signal for an increasing amount of polymer.

From a quantitative point of view, it is now relevant to correlate the secondary-ion yield to the degree of surface coverage (Figure 13). A linear correlation is observed between the secondary-ion yield and the degree of surface coverage (with one outlier point at 100% normalized secondary-ion yield excluded in the linear regression for PVC). The slope of the PVC line is 0.96 ($R = 0.997$), and the intercept is zero. The slope of the PMMA line is 1.03 ($R = 0.998$), and the intercept is -18% . The reason that the PMMA curve does not have an intercept of zero is probably due to an isobaric background signal. These are the desired calibration curves for the lateral quantification.

Substrate signals were also monitored for the varying polymer surface coverages. The expected approximately linear decrease in the intensity of the secondary ions originating from the substrate with polymer coverage was observed, but as this did not provide additional information about the coverage in comparison to that obtained from the polymer secondary ions, we have not presented these data.

4. Conclusions

For the multilayers, the sputter profiles for PVC and PMMA using Si^+ as a marker were observed to have different shapes, probably as a result of material-dependent sputter conditions. The maximum silicon signal intensities from the two polymer-coated substrates were observed to differ by a factor of 4, which we believe to be due to measured differences in the concentration of non-silicon species implanted in the silicon substrate during the sputter process (matrix effect). A plot of the layer thickness versus the sputter time produces a calibration curve for the vertical quantification. From the nonlinearity, we

conclude that the sputter rates are not constant (i.e., the sputter rate varies with the integrated ion fluence, probably because of a combination of insufficient charge compensation and chemical modification of the polymer induced by the sputter process, e.g., cross-linking and/or bond cleavage, or because of interlayer mixing).

PVC and PMMA both form domains in the submonolayer concentration range. In the intermediate concentration range between domain formation and complete surface coverage, networks form. TOF-SIMS imaging was observed to be inferior to AFM imaging with regard to determining the lateral distribution of polymers on silicon surfaces.

In the submonolayer concentration range, XPS as well as TOF-SIMS signals originating from the polymer are observed to increase slightly for an increase in polymer concentration. At the concentration corresponding to incipient network formation, the TOF-SIMS and XPS signals are observed to increase drastically. The same trend is observed for the degree of surface coverage (measured by AFM). By calculating the effective thickness in the submonolayer concentration range, we conclude that there is a simple relation between the concentration and the amount of polymer deposited on the surface (i.e. there is no drastic increase in the amount deposited on the surface at the concentration that corresponds to incipient network formation). At low concentrations, the polymer is distributed in the plane of the substrate as well as perpendicular to the substrate, resulting in relatively thick domains distributed over a limited surface area. At higher concentrations, when the network starts to form, it is more favorable to distribute the polymer in the lateral plane rather than perpendicular to the surface, resulting in a relatively thin network with a large degree of surface coverage.

In summary, we conclude that TOF-SIMS analysis is a viable methodology with which to study the surface morphology of ultrathin polymer coatings. We found the correlation between surface coverage and secondary-ion yield to be close to linear for the two model polymers investigated. Three main advantages of using TOF-SIMS over the traditionally applied techniques of XPS and AFM for these types of studies were identified: (i)

Analysis time is reduced by several orders of magnitude (typically tens of seconds for TOF-SIMS and tens of minutes for XPS and AFM). (ii) TOF-SIMS provides significantly higher sensitivity than XPS at low surface coverage, and the area-averaging ability of TOF-SIMS is superior to that of AFM. (iii) The surface specificity of TOF-SIMS is markedly higher than that of XPS. The depth of thicker polymer coatings may be probed by TOF-SIMS depth profiling. However, we observed a nonlinear correlation between layer thickness and sputter time due to a decrease in sputter rate with increasing thickness. This indicates that TOF-SIMS depth profiling of polymers is strongly system-dependent; consequently, calibration curves should be determined for each combination of materials, and layer thicknesses should be investigated.

Acknowledgment. Dr. Walther Batsberg Pedersen is gratefully acknowledged for helpful discussions and Dr. José Augusto Dâmaso Condeço is gratefully acknowledged for help with part of the AFM image handling.

References and Notes

- (1) *TOF-SIMS Surface Analysis by Mass Spectrometry*; Vickerman, J. C., Briggs, D., Eds.; IM Publications and SurfaceSpectra Limited: 2001.
- (2) Briggs, D. *Surface Analysis of Polymers by XPS and Static SIMS*; Cambridge University Press: Cambridge, U.K., 1998.
- (3) Galuska, A. A. *Surf. Interface Anal.* **1994**, *21*, 703–710.
- (4) Galuska, A. A. *Surf. Interface Anal.* **1996**, *24*, 380–388.
- (5) Galuska, A. A. *Surf. Interface Anal.* **1997**, *25*, 1–4.
- (6) Li, L.; Ng, K. M.; Chan, C. M.; Feng, J. Y.; Zeng, X. M.; Weng, L. T. *Macromolecules* **2000**, *33*, 5588–5592.
- (7) Jackson S. T.; Short, R. D. *J. Mater. Chem.* **1992**, *2*, 259–260.
- (8) Briggs, D. *Spectrosc. Eur.* **1993**, *5*, 8.
- (9) Briggs, D. *Surface Analysis of Polymers by XPS and Static SIMS*; Cambridge University Press: Cambridge, U.K., 1998; p 182.
- (10) Briggs, D.; Fletcher, I. W.; Reichlmaier, S.; AguloSanchez, J. L.; Short, R. D. *Surf. Interface Anal.* **1996**, *24*, 419–421.
- (11) Leeson, A. M.; Alexander, M. R.; Short, R. D.; Hearn, M. J.; Briggs, D. *Int. J. Polymer Anal. Charact.* **1997**, *4*, 133–151.
- (12) Muddiman, D. C.; Brockman, A. H.; Proctor, A.; Houalla, M.; Hercules, D. M. *J. Phys. Chem.* **1994**, *98*, 11570–11575.
- (13) Dobbs, D. A.; Bergman, R. G.; Theopold, K. H. *Chem. Eng. News* **1990**, *68*, 2.
- (14) Delcorte, A.; Bertrand, P.; Arys, X.; Jonas, A.; Wischerhoff, E.; Mayer, B.; Laschewsky, A. *Surf. Sci.* **1996**, *366*, 149–165.